Journal of Power Sources 192 (2009) 175–179

Contents lists available at ScienceDirect

Journal of Power Sources

journal homepage: www.elsevier.com/locate/jpowsour

Short communication

The effect of doping in the electrochemical performance of $(Ln_{1-x}M_x)FeO_{3-\delta}$ SOFC cathodes

Karmele Vidal[a], Lide M. Rodríguez-Martínez[b], Luis Ortega-San-Martin[c], Ana Martínez-Amesti[a], María Luisa Nó[a], Teófilo Rojo[a], Ander Laresgoiti[b], María Isabel Arriortua[a,*]

[a] Facultad de Ciencia y Tecnología, Universidad del País Vasco/Euskal Herriko Unibertsitatea, Apdo. 644, E-48080 Bilbao, Spain
[b] Ikerlan, Centro Tecnológico, Parque Tecnológico de Alava, Juan de la Cierva 1, Miñano 01510, Álava, Spain
[c] Instituto de Ciencia de Materiales de Aragón, C.S.I.C.-Universidad de Zaragoza, C/María de Luna, 3, 50018 Zaragoza, Spain

ARTICLE INFO

Article history:
Received 15 October 2008
Received in revised form 9 December 2008
Accepted 9 December 2008
Available online 31 December 2008

Keywords:
LSF
Perovskite
SOFC cathodes
Electrochemical performance
A-site

ABSTRACT

A family of iron perovskites with the general formula $AFeO_{3-\delta}$ ($A = Ln_{1-x}M_x$; Ln = La, Nd and/or Pr; M = Sr or/and Ca) has been prepared keeping fixed the A cation radius $\langle r_A \rangle$ and cation size mismatch to isolate the effect of divalent dopant concentration from the A-cation steric effects. The electrochemical behaviour of these compounds for their application as SOFC cathodes was evaluated by using *I–V* curve measurements and ac impedance spectroscopy over three electrodes electrolyte supported cells processed under identical conditions. In contrast with the bulk behaviour, trends are more difficult to observe due to microstructural effects, but results seem to indicate that the doping level, *x*, does not influence in a significant way the electrochemical performance of iron perovskites with identical $\langle r_A \rangle$ and $\sigma^2(r_A)$.

1. Introduction

Classical LSM ($La_{1-x}Sr_xMnO_3$) compounds have shown good and stable performance as cathode materials in Solid Oxide Fuel Cells (SOFCs) operating at temperatures above 800 °C, however their performance decreases rapidly as the temperature decreases [1]. Cobalt containing perovskite oxides usually exhibit higher ionic conductivities than LSM due to a greater concentration of oxygen vacancies. Nevertheless, their thermal expansion coefficients (TECs) are much larger than those corresponding to the electrolytes [2,3]. Iron perovskites such as LSF ($La_{1-x}Sr_xFeO_3$) are also good candidates as SOFC cathodes [4] showing a better-matched TEC while maintaining the high mixed conductivity and good catalytic activity for oxygen reduction. In addition, LSF perovskites tend to react more slowly with the typical yttrium-stabilized zirconia (YSZ) electrolyte than LSM and LSC compounds at the operating temperature. Then, the LSF cathodes give promising high power outputs and long-term stability.

The present $(Ln_{1-x}M_x)FeO_{3-\delta}$ system has been chosen to study the systematic effect on their properties of different parameters that control the A-site of the perovskite structure ($A = Ln_{1-x}M_x$). The A-site is generally composed by combinations of trivalent lanthanide (Ln = La, Pr, Nd, Sm, Gd) and divalent alkaline-earth cations (M = Ca, Sr, Ba) which produce different average sizes, $\langle r_A \rangle$, and charge of the A-site. This directly affects the oxidation state and average size of the B-site cation (Fe for this case), given by the doping level *x*. Apart from the average A size and doping, there is a third factor that affects the properties of perovskite materials: the variance of the A-cation radius distribution, $\sigma^2(r_A)$, that arises from the size mismatch of the cations occupying the A-site. The effects of the size mismatch and disorder have been studied in $AMnO_3$ perovskites [5] and extended to other systems such as A_2CuO_4 superconductors [6], and $ATiO_3$ [7] and $ACoO_3$ [8] perovskites. These studies have shown interesting trends with the A-site parameters in several properties such as the magnetoresistive response, superconducting critical temperatures, and ferromagnetic Tc, for example.

Following these studies it has been considered interesting to carry out similar studies for iron perovskites that have properties of potential use as SOFC cathodes. In this sense, we aim to study separately the effects of doping *x*, average size $\langle r_A \rangle$, and disorder $\sigma^2(r_A)$ over the structure and properties of a series of $(Ln_{1-x}M_x)FeO_{3-\delta}$ perovskite oxides. In a previous work we observed that when doping level *x* is isolated from the other two parameters several trends in the structure, microstructure, and conductivity of the samples in bulk could be clearly distinguished [9]. To our knowledge, that has been the first time that the effect of the parameter *x* has been

* Corresponding author. Tel.: +34 946 015 801; fax: +34 946 013 500.
E-mail addresses: karmele.vidal@ehu.es (K. Vidal), maribel.arriortua@ehu.es (M.I. Arriortua).

0378-7753/$ – see front matter © 2009 Elsevier B.V. All rights reserved.
doi:10.1016/j.jpowsour.2008.12.034

Table 1
Particle size distribution analysis of the prepared $Ln_{1-x}M_xFeO_{3-\delta}$ iron oxide perovskites.

x	Composition	$\langle r_A \rangle$ (Å)	σ^2 (Å^2)	d_{10} (μm)*	d_{50} (μm)*	d_{90} (μm)*
0.2	$La_{0.50}Pr_{0.30}Sr_{0.20}FeO_{3-\delta}$	1.219	0.0026	0.54	1.56	6.16
0.3	$La_{0.40}Nd_{0.30}Sr_{0.23}Ca_{0.07}FeO_{3-\delta}$	1.219	0.0030	0.63	1.83	6.54
0.4	$La_{0.20}Pr_{0.40}Sr_{0.26}Ca_{0.14}FeO_{3-\delta}$	1.221	0.0030	0.56	1.56	4.46
0.5	$La_{0.19}Pr_{0.31}Sr_{0.26}Ca_{0.24}FeO_{3-\delta}$	1.220	0.0030	0.58	1.72	7.09
0.6	$La_{0.19}Pr_{0.21}Sr_{0.26}Ca_{0.34}FeO_{3-\delta}$	1.220	0.0030	0.57	1.53	5.03
0.7	$La_{0.18}Pr_{0.12}Sr_{0.26}Ca_{044}FeO_{3-\delta}$	1.220	0.0030	0.51	1.76	7.24
0.8	$La_{0.20}Sr_{0.25}Ca_{0.55}FeO_{3-\delta}$	1.220	0.0029	0.77	3.44	15.22

Nominal compositions, mean ionic radius, cation size disorder and doping level x are given.
* d_i indicates that the i percent of the particles present a size smaller than the value given under d_i.

isolated from the effects of the other chemical parameters. In order to continue that study, here we investigate the effect of the variation of the doping level x on the microstructure and electrochemical properties of the same perovskites applied as cathodes in electrolyte supported SOFC cells. This has been achieved by keeping the average size, $\langle r_A \rangle$, and size mismatch, $\sigma^2(r_A)$, constant throughout the whole series of compositions prepared. In order to allow for suitable combinations of A-cations over the whole doping range $0.2 \leq x \leq 0.8$, the fixed values of $\langle r_A \rangle$, and $\sigma^2(r_A)$ chosen were 1.22 Å and 0.003 Å^2, respectively.

2. Experimental

Perovskites of general formula $(Ln_{1-x}M_x)FeO_{3-\delta}$ (Ln = La, Nd, Pr; M = Sr, Ca) with $0.2 \leq x \leq 0.8$ have been synthesised by conventional ceramic solid state reaction under identical synthetic conditions. These conditions and the room temperature X-ray powder diffraction, compositional analysis, bulk microstructure, and dc conductivity data on sintered rectangular bars of these compounds in bulk have been reported elsewhere [9].

The previously characterised powders were ball milled under identical conditions for 24 h and measured using a Malvern Mastersizer X particle size analyser. Each of these powders was then deposited by colloidal spraying onto scandium stabilized zirconium electrolyte disks (SSZ, Daiichi Kiganso Kagaku Kogyo Co., DKKK, 150 μm thickness manufactured by tape casting by Kerafol). A samarium doped cerium oxide (SDC) (Praxair, Surface Technologies, Combustion Spray Pyrolysis, 99.9%, surface area 14.15 m^2 g^{-1}, d_{50} = 0.6 μm) barrier layer was sprayed and fired at 1100 °C between the electrolyte and the cathode in order to prevent the formation of phases that lead to electrode degradation [10,11]. Cathode was subsequently fired at 1100 °C for 2 h. A cermet anode of Ni–SSZ (prepared from a 50:50 volume ratio mixture of NiO, Sigma–Aldrich and SSZ) was previously applied to SSZ discs and fired at 1250 °C. Pt paste and mesh were used for the pseudoreference electrode and for current collection.

Electrochemical impedance spectroscopy measurements were performed using a Solartron 1260 Frequency Response Analyser coupled to a 1286 Electrochemical Interface. The impedance spectra of the three electrodes cells were recorded at OCP, 100 and 300 mA with a 10 mV ac signal amplitude over the frequency range 10^6–0.01 Hz at 700 and 800 °C. The cathode was exposed to ambient air and the anode to humidified hydrogen at a flow rate of 100 ml min^{-1}. Current–voltage (*IV*) measurements have also been performed between 700 and 800 °C.

Images of the microstructure and cross section of button cells were taken after electrochemical testing using a JEOL JSM 6400 scanning electron microscope (SEM) at room temperature.

3. Results and discussion

The results from particle size analysis after ball milling are reported in Table 1, together with the compositions of the $(Ln_{1-x}M_x)FeO_{3-\delta}$ powders and their corresponding values of doping x, average size $\langle r_A \rangle$, and size mismatch $\sigma^2(r_A)$. The particle size distribution analysis of these powders prior to their application onto cells indicates that powders between x = 0.2 and 0.7 present comparable fractions and particle sizes, while sample x = 0.8 posses significantly larger sizes, particularly at d_{50} and d_{90}.

Typical scanning electron microscopy images of working and counter electrodes deposited by colloidal spraying are shown in Fig. 1. The SDC barrier layers are normally between 4 and 6 μm, whereas the $Ln_{1-x}M_xFeO_{3-\delta}$ cathode layers were between 20 and 30 μm (Fig. 1a). The anode layers deposited were between 30 and 40 μm, as shown in Fig. 1b. On the other hand, details of cathode microstructures as a function of doping are summarised in Fig. 2. On average, these cathodes show similar grain sizes, typically under 1 μm. This is consistent with the homogeneity of the

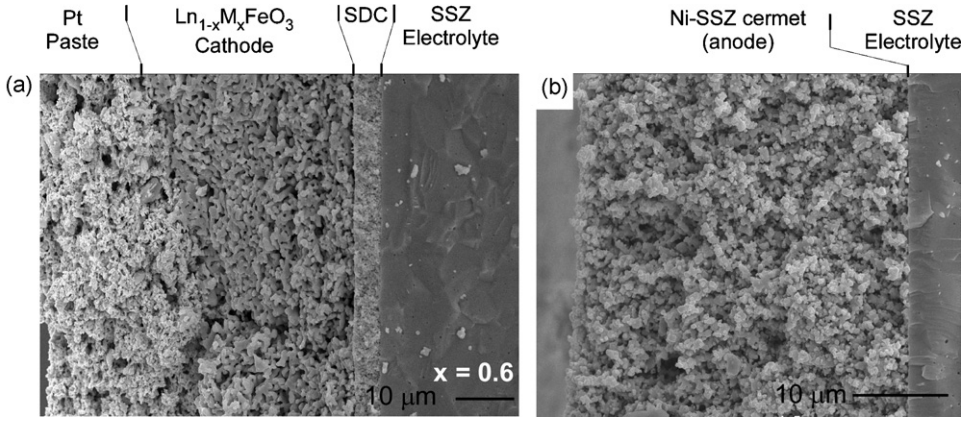

Fig. 1. Scanning electron microscopy (SEM) images obtained at the same magnification for (a) cathode side cross section, and (b) anode side cross section of sample with x = 0.6.

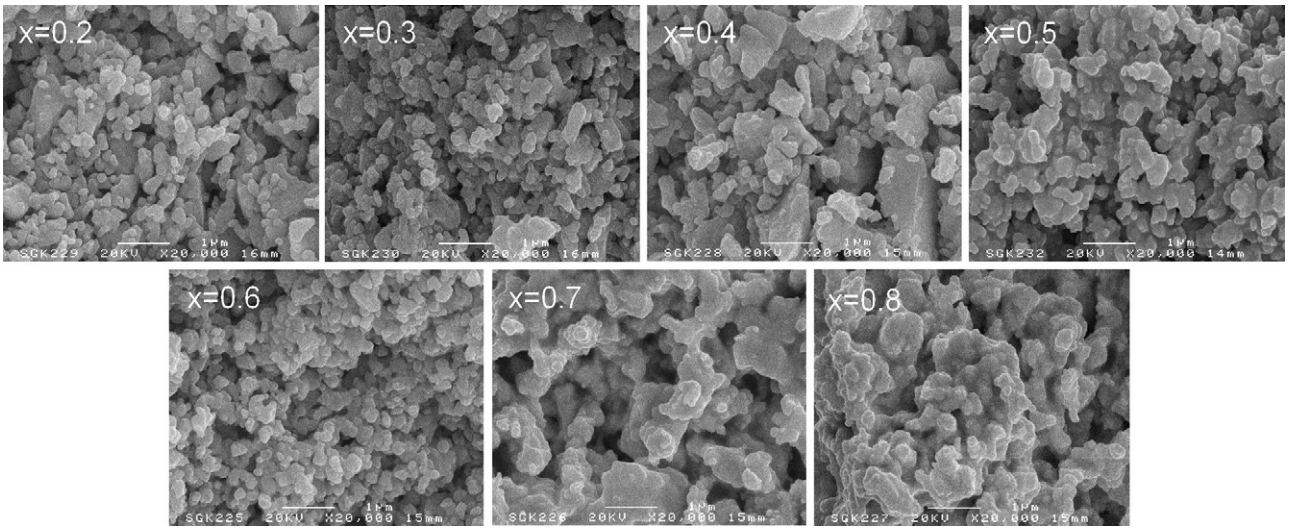

Fig. 2. Details of cathode microstructures for all $Ln_{1-x}M_xFeO_{3-\delta}$ tested cells obtained by SEM under the same magnification.

starting powders. A slight increase of grain size as the doping level x increases can also be observed, which is consistent although less dramatic than the increase observed by SEM analysis performed on bulk surface polycrystalline bars [9]. This trend has been associated to a change in melting point of the samples with increase in alkaline-earth cation content [12–14] as the end members $CaFeO_3$ and $SrFeO_3$ have lower melting points than $LaFeO_3$ and $PrFeO_3$. This increase is particularly evident in $x = 0.8$ phase, in agreement with the bigger grain size of the raw powder (Table 1).

Electrochemical impedance spectroscopy measurements for all cathodes at 700 and 800 °C at open circuit voltage (OCP) and under a current of 100 and 300 mA were measured using an external pseudoreference electrode (Fig. 3). The ohmic contributions, which are mainly attributed to the electrolyte, have been subtracted for clarity. Hence, the evolution of cathode polarisation resistances (R_p) as a function of doping can be observed at different current conditions and for both sets of temperatures.

In most cases, several arcs are present for each impedance spectrum, indicating the contributions from various processes towards the electrode reaction. The high frequency arc is usually associated with the charge transfer processes [15,16]. The lower frequency arc is usually attributed to oxygen adsorption and diffusion at the cathode surface. The existence of additional arcs can be due to gas diffusion, activated processes due to impurities, phase segregation, etc.

In any case, there is a clear dependence of cathode polarisation resistance upon current load in most cases at both temperatures. This dependence is manifested as a sharp reduction of R_p as the applied current is increased. In general, this is usually associated to effects such as an improvement in grain adherence at the

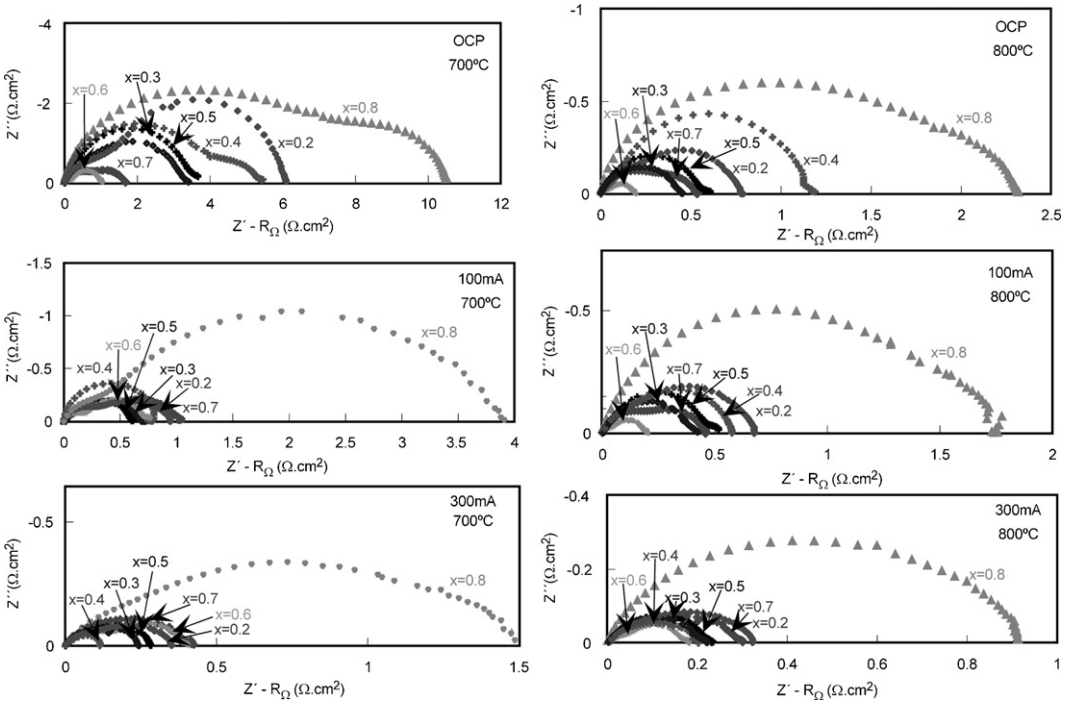

Fig. 3. Nyquist plots of the electrode response at 700 and 800 °C for all compositions measured at OCP, 100 and 300 mA. Serial resistance was subtracted from all spectra for clarity.

cathode–electrolyte interface, and sintering effects due to current flow or formation of mixed conducting zones due to partial cathode reduction at high polarisation [17]. Once current is applied, most cathodes behave in a similar way, with differences amongst them being more significant when measured at open circuit potential. Generally, higher resistances correspond to compounds with lowest and highest doping levels, which might be related to their lower bulk conductivity as shown in the previous study [9]. In that study it was clearly observed that samples with intermediate doping levels showed higher conductivities. In the present case those differences are less marked all being within comparable R_p values. The half-cell corresponding to the highly doped sample $x = 0.8$ shows comparatively very high polarisation resistances under all the experimental conditions considered. This may be due to the anomalously large particle sizes for this sample and the increased grain growth observed for this sample as reported in Table 1 and Fig. 3. This is a clear indication that both particle sizes and microstructure are crucial parameters that affect cathode performance.

Current–voltage measurements at 700 and 800 °C for cathode overpotentials are summarised in Fig. 4. The trends upon doping are in good agreement with those observed by impedance measurements. In both temperature regimes the best performance corresponds to sample with $x = 0.6$ whereas the least interesting performance clearly corresponds to sample with $x = 0.8$. All the remaining compositions show similar behaviour, values lying within a narrow range.

Available literature about the specific effects of the A-site substitution on the electrochemical performance of perovskites as SOFC cathodes is scarce and inconclusive. While Sakaki et al. [18] consider that the A-site substitution does not affect these properties

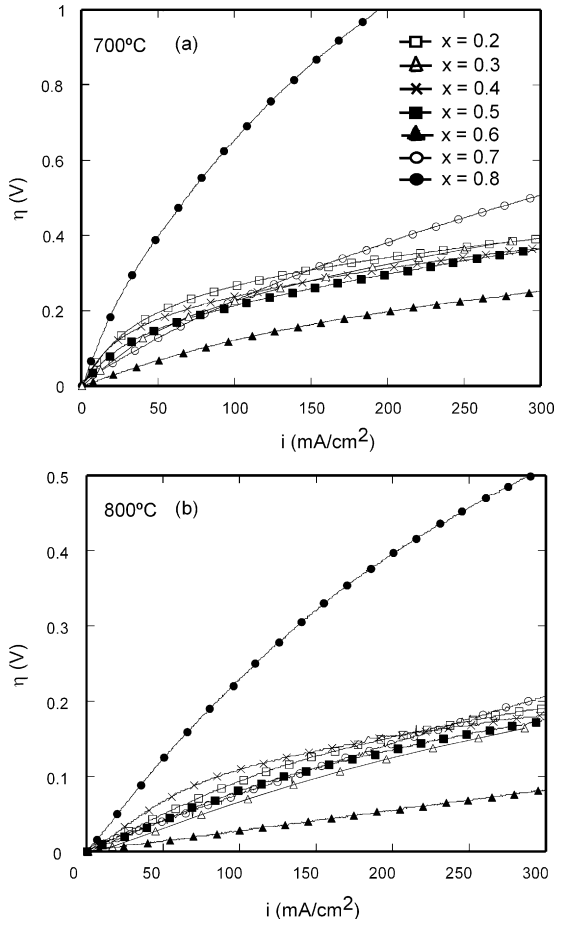

Fig. 4. IV measurements of $Ln_{1-x}M_xFeO_3$ cathodes at (a) 700, and (b) 800 °C.

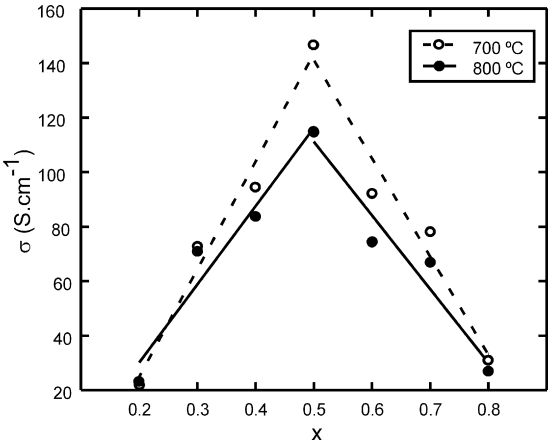

Fig. 5. Bulk 4-probe corrected conductivity measurements on sintered polycrystalline bars as a function of doping level at 700 and 800 °C (see also Ref. [9]).

some authors have found a decrease in resistance upon doping up to $x = 0.5$ and a subsequent increase for higher doping values [19,20]. This latter trend is in good agreement with the results from bulk conductivity measurements (corrected for porosity [21]) for our $Ln_{1-x}M_xFeO_{3-\delta}$ polycrystalline bars, which are shown in Fig. 5.

Systematic studies focused on B-site transition metal substitution show a significant effect of the B-site cation in their electrochemical performance [22,23].

From the results reported in this study, the isolated effect of doping provides lowest polarisation resistances at intermediate doping levels, although the effect is less marked than expected from bulk measurements, probably due to microstructural effects which dominate performance over compositional effects. However, we consider that the observed trends with doping are real, as similar comparative studies have been carried out in our group isolating the effect of A-cation size, $\langle r_A \rangle$, and cation size mismatch, $\sigma^2(r_A)$ [24]. In this sense we have observed that when used as cathodes under identical synthesis, processing and experimental conditions, systematic trends can be easily seen with $\langle r_A \rangle$ and $\sigma^2(r_A)$, while doping in the A-site has a lesser influence. We understand that the particle size distribution of starting powders, as shown in Table 1, are not ideal for their use as SOFC cathodes. The limitations come from the fact that all the basic characterisations in bulk and their application in electrolyte supported cells have been performed with powders prepared in one batch. The shortage of these powders made it practically impossible to achieve the required particle size reduction, but allowed us to obtain results from different samples under identical experimental conditions.

Mizusaki et al. [25] showed that the reaction rate for coarse particle sizes (1–3 μm) in $La_{0.6}Ca_{0.4}MnO_3$ was practically independent of cathode thickness but proportional to the TPB length. Thus, Haart et al. [26] concluded that the cathode polarisation for $La_{0.85}Sr_{0.15}MnO_3$ prepared by dip coating did not vary significantly either with the microstructure or cathode thickness. However, Sasaki et al. [27] related the cathode performance of $La_{0.85}Sr_{0.15}MnO_3$ prepared by screen printing with the TPB length and cathode thickness, giving an optimum value of 25 μm. They also observed that cathodes with narrower particle size distributions yield lower R_p values, in agreement with results from van Heuveln [28].

All this indicates that there exist multiple factors despite compositions that markedly affect cathode performance. In this study, the synthesis, processing and firing conditions have been kept identical for all the compositions and we believe there are further variables that affect the electrochemical study, such as the intrinsic microstructure of the cathode material, related to the different

melting points of the A-site substituting cations, which affect the grain growth. For this and other reasons, we believe the separate effect of doping in the performance of perovskites as SOFC cathodes needs further detailed investigation, through techniques capable of separating microstructural effects from compositional effects.

4. Conclusions

The effect of doping level x in the electrochemical performance of iron $Ln_{1-x}M_xFeO_{3-\delta}$ perovskites with fixed values of $\langle r_A \rangle$ (1.22 Å) and $\sigma^2(r_A)$ (0.003 Å^2) has been studied on electrolyte supported SOFC cells. SEM analysis of the tested cathodes shows a slight increase of grain growth as the doping level x increases, which is consistent although less dramatic than the results observed for bulk surface polycrystalline bars. Electrochemical impedance spectroscopy measurements show a decrease in the polarization resistance, R_p, as the applied current increases which indicates the activation of the cathode materials. The highly doped sample $x = 0.8$ shows high polarisation resistances under all the experimental conditions considered, that may be due to the anomalously large particle sizes for this sample.

Overall, best performing cathodes correspond to the intermediate doping levels but the variations in R_p are not significant over the studied $0.2 \leq x \leq 0.8$ range. Microstructural effects, intrinsic and extrinsic to composition, are key factors affecting cathode performance that should carefully be considered to successfully isolate the effect of composition.

Acknowledgments

This work has been financially supported by the "Departamento de Industria del Gobierno Vasco/Eusko Jaurlaritza", within the strategic actions in Microenergy (GARAZI project, ETORTEK 2007-2009, SAIOTEK 2007 programmes, MEC proyect MAT 2007-66737). The authors thank the technicians of SGIker, financed by the "National Program for the Promotion of Human Resources within the National Plan of Scientific Research, Development and Innovation – "Ministerio de Ciencia y Tecnología", "Fondo Social Europeo (FSE)" and "Gobierno Vasco/Eusko Jaurlaritza, Dirección de Política Científica" for the X-ray diffraction and SEM measurements. K. Vidal also acknowledges the Basque Government for a Doctoral Fellowship, respectively.

References

[1] S.J. Skinner, Int. J. Inorg. Mater. 3 (2001) 113.
[2] G. Zhu, X. Fang, C. Xia, X. Liu, Ceram. Int. 31 (2005) 115.
[3] N.Q. Minh, J. Am. Ceram. Soc. 76 (1993) 563.
[4] S.P. Simmer, J.F. Bonnett, N.L. Canfield, K.D. Meinhardt, J.P. Shelton, V.L. Sprenkle, J.W. Stevenson, J. Power Sources 113 (2003) 1.
[5] L.M. Rodriguez-Martinez, J.P. Attfield, Phys. Rev. B 54 (1996) R15622.
[6] J.P. Attfield, A.L. Kharlanov, J.A. McAllister, Nature 394 (1998) 157.
[7] D.C. Sinclair, J.P. Attfield, Chem. Comm. 16 (1999) 1497.
[8] P.V. Vanitha, A. Arulraj, P.N. Santhosh, C.N.R. Rao, Chem. Mater. 12 (2000) 1666.
[9] K. Vidal, L.M. Rodríguez-Martínez, L. Ortega-San-Martin, E. Díez-Linaza, M.L. Nó, T. Rojo, A. Laresgoiti, M.I. Arriortua, Solid State Ionics 178 (2007) 1310.
[10] E. Ivers-Tiffee, A. Webe, K. Schmid, Volker Krebs, Solid State Ionics 174 (2004) 223.
[11] A. Weber, R. Manner, E. Ivers-Tiffee, Denki Kagaku 64 (1996) 582.
[12] V.V. Kharton, A.L. Shaulo, A.P. Viskup, M. Avdeev, A.A. Yaremchenko, M.V. Patrakeev, A.I. Kurbakov, E.N. Naumovich, F.M.B. Marques, Solid State Ionics 150 (2002) 229.
[13] Y.C. Liou, Mater. Sci. Eng., B, Solid-State Mater. Adv. Technol. 108 (2004) 278.
[14] Y.C. Liou, Ceram. Int. 30 (2004) 667.
[15] F. Qiang, K.N. Sun, N.Q. Zhang, X.D. Zhu, S.R. Le, D.R. Zhou, J. Power Sources 168 (2007) 338.
[16] K. An, K.L. Reifsnider, C.Y. Gao, J. Power Sources 158 (2006) 254.
[17] T. Kenjo, S. Osawa, K. Fujikawa, J. Electrochem. Soc. 138 (1991) 349.
[18] Y. Sakaki, Y. Takeda, A. Kato, N. Imanishi, O. Yamamoto, M. Hattori, M. Lio, Y. Esaki, Solid State Ionics 118 (1999) 187.
[19] T. Ishihara, T. Kudo, H. Matsuda, Y. Takita, J. Electrochem. Soc. 142 (1995) 1519.
[20] H.-K. Lee, Mater. Chem. Phys. 77 (2002) 639.
[21] W.C. Hagel, J. Am. Ceram. Soc. 48 (1965) 70.
[22] A. Mai, V.A.C. Haanappel, S. Uhlenbruck, F. Tietz, D. Stöver, Solid State Ionics 176 (2005) 1341.
[23] H. Lv, B.-Y. Zhao, Y.-J. Wu, G. Sun, G. Chen, K.-A. Hu, Mater. Res. Bull 42 (2007) 1999.
[24] K. Vidal, PhD Thesis, Basque Country University (UPV/EHU)-Ikerlan, 2008.
[25] J. Mizusaki, H. Tagawa, K. Tsuneyoshi, A. Sawata, J. Electrochem. Soc. 138 (1991) 1867.
[26] L.G.J. de Haart, R.A. Kuipers, K.J. de Vries, A.J. Burggraf, J. Electrochem. Soc. 138 (1991) 1970–1975.
[27] K. Sasaki, J.P. Wurth, M. Godickemeier, A. Mitterdorfer, L.J. Gaukler, in: M. Dokiya, H. Yamamoto, H. Tagawa, S.C. Singhal (Eds.), Proceedings of the Fourth Int. Symp. on SOFC, Electrochem Soc. Proc. 95 (1995) 625.
[28] F. van Heuveln. PhD thesis, University of Twente-ECN, 1997.